CrossMark

RESEARCH ARTICLE

Photobiomodulation-induced changes in a monkey model of Parkinson's disease: changes in tyrosine hydroxylase cells and GDNF expression in the striatum

Nabil El Massri[1] · Ana P. Lemgruber[1] · Isobel J. Rowe[1] · Cécile Moro[2] ·
Napoleon Torres[2] · Florian Reinhart[2] · Claude Chabrol[2] · Alim-Louis Benabid[2] ·
John Mitrofanis[1]

Abstract Intracranial application of red to infrared light, known also as photobiomodulation (PBM), has been shown to improve locomotor activity and to neuroprotect midbrain dopaminergic cells in rodent and monkey models of Parkinson's disease. In this study, we explored whether PBM has any influence on the number of tyrosine hydroxylase (TH)[+]cells and the expression of GDNF (glial-derived neurotrophic factor) in the striatum. Striatal sections of MPTP (1-methyl-4-phenyl-1,2,3,6-tetrahydropyridine)-treated mice and monkeys and 6-hydroxydopamine (6OHDA)-lesioned rats that had PBM optical fibres implanted intracranially (or not) were processed for immunohistochemistry (all species) or western blot analysis (monkeys). In our MPTP monkey model, which showed a clear loss in striatal dopaminergic terminations, PBM generated a striking increase in striatal TH[+] cell number, 60% higher compared to MPTP monkeys not treated with PBM and 80% higher than controls. This increase was not evident in our MPTP mouse and 6OHDA rat models, both of which showed minimal loss in striatal terminations. In monkeys, the increase in striatal TH[+] cell number in MPTP-PBM cases was accompanied by similar increases in GDNF expression, as determined from western blots, from MPTP and control cases. In summary, these results offer insights into the mechanisms by which PBM generates its beneficial effects, potentially with the use of trophic factors, such as GDNF.

Introduction

It is well known that the striatum receives rich terminal inputs from the dopaminergic cells of the substantia nigra pars compacta (SNc; Parent and Hazrati 1995; Blandini et al. 2000). A less well known feature is that the striatum itself houses a resident population of putative dopaminergic, tyrosine hydroxylase (TH) containing, cells (Dubach et al. 1987; Tashiro et al. 1989; Betarbet et al. 1997). Many of these form part of the smaller aspiny interneurone population of the striatum (Dubach et al. 1987; Betarbet et al. 1997). In truth, their existence would not have generated widespread interest, except for the observation that their number increases after parkinsonian insult (Betarbet et al. 1997; Meredith et al. 1999; Porritt et al. 2000; Palfi et al. 2002; Cossette et al. 2005; Mazloom and Smith 2006; Tandè et al. 2006; Sebastian et al. 2007; Ünal et al. 2013; Depboylu 2014; Xenias et al. 2015). This increase is considered a compensatory response to the massive depletion of dopamine levels in the deafferentated striatum (Betarbet et al. 1997; Porritt et al. 2000; Cossette et al. 2005).

Several studies have explored the issue of whether the striatal TH^{+} cells are dopaminergic. In rodents, many cells have been reported to not contain dopamine nor the key enzymes in dopamine production, for example vesicular monoamine transporter-2 (VMaT2) and/or the dopamine transporter molecule (DAT; Meredith et al. 1999; Depboylu 2014; Xenias et al. 2015). Further, no striatal TH^{+} cells in rodents appear to express the phosphorylated forms of TH (ie, S40, S31 and S19), which indicates a low functional TH activity (Depboylu 2014). By contrast, many striatal

✉ John Mitrofanis
john.mitrofanis@sydney.edu.au

[1] Department of Anatomy F13, University of Sydney, Sydney 2006, Australia

[2] University of Grenoble Alpes, CEA, LETI, CLINATEC, MINATEC Campus, 38000 Grenoble, France
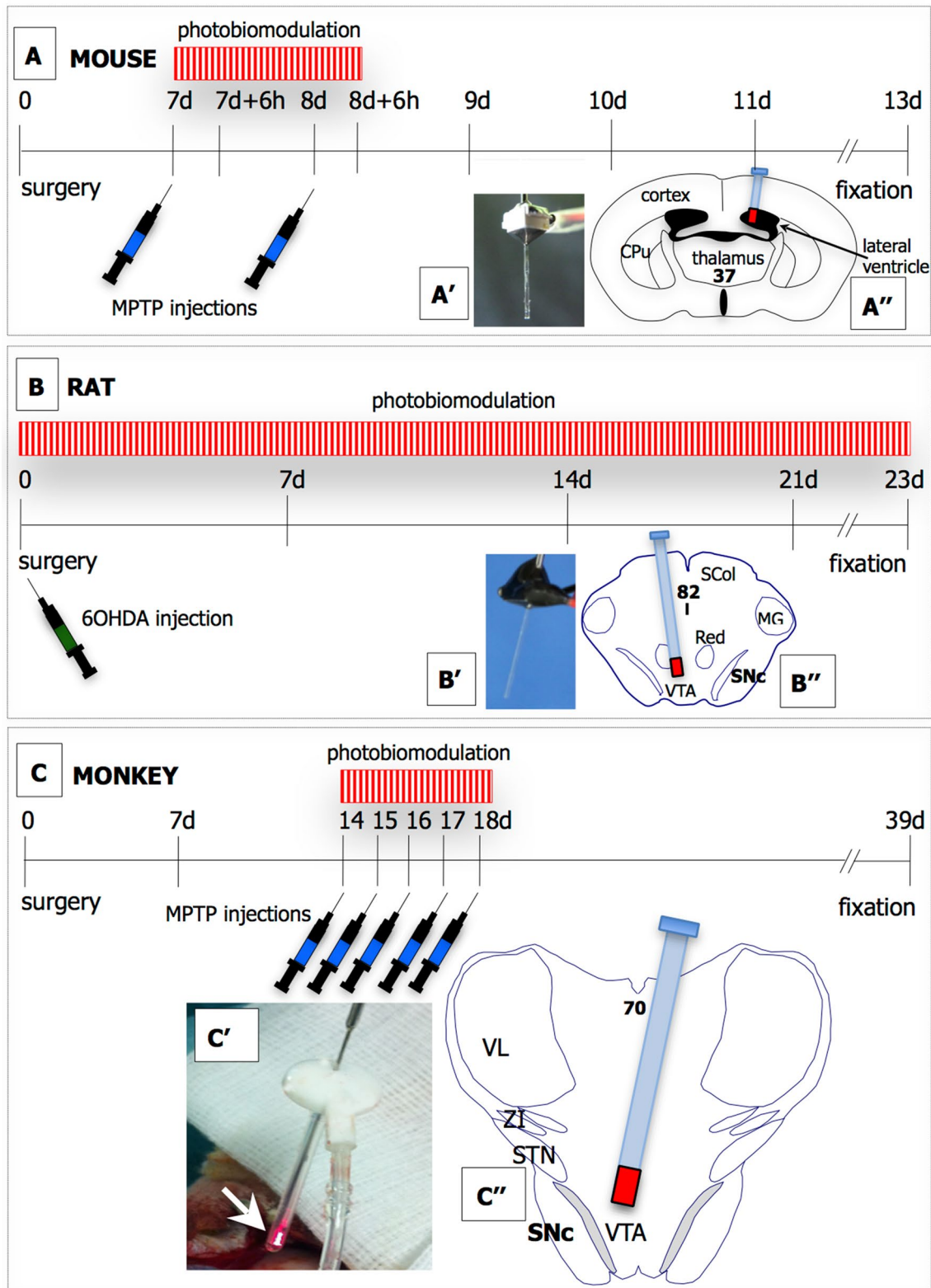
TH^{+} cells in monkeys and humans have been reported to have DAT[+], although many cells lack VMaT2 (see Betarbet et al. 1997; Porritt et al. 2000; Palfi et al. 2002; Cossette et al. 2005; Weihe et al. 2006; Tandè et al. 2006).

Notwithstanding possible species differences, there is general agreement that a loss of dopaminergic inputs to the striatum triggers the expression of normally quiescent TH enzyme in many small striatal cells.

◄Fig. 1 Outline of the experimental design of this study. **a** Mice: a week after optical fibre implant (*A′*) into the lateral ventricle (*A″*), animals had two injections of MPTP (50 mg/kg) or saline over 24 h. Soon after the first injection, the PBM optical fibre was turned-on (*red striped box*) and remained on up until 6 h after the last injection; the device in non-PBM-treated animals was not turned-on during this period. The *number* in the schematic diagram of coronal section (*A″*) corresponds to plate in mouse atlas (Paxinos and Franklin 2001). **b** Rats: immediately after 6OHDA or saline injection into the striatum, animals had an optical fibre implant (*B′*) into a midline midbrain region (*B″*). Soon after the implant, the PBM optical fibre was turned-on (*red striped box*) and remained on up until perfusion on 23 days; the device in non-PBM-treated animals was not turned-on during this period. The number in the schematic diagram of coronal section (*B″*) corresponds to plate in rat atlas (Paxinos and Watson 2005). **c** Monkeys: 2 weeks after optical fibre implant (*C′*) into a midline midbrain region (*C″*), animals had five injections of MPTP (1.5 mg/kg) or not over 24 h. Soon after the first injection, the PBM optical fibre was turned-on (*red striped box*) and remained on up until 24 h after the last injection; the device in non-PBM-treated animals was not turned-on during this period. The *number* in the schematic diagram of coronal section (*C″*) corresponds to plate in monkey atlas (Paxinos et al. 1998)

In this context, several studies have reported that when glial derived neurotrophic factor (GDNF) is introduced to the striatum of MPTP-treated monkeys, either by gene delivery using a lentiviral vector (Palfi et al. 2002) or by a carotid body graft (Sebastian et al. 2007), there is an increase in the number of striatal TH$^+$ cells. Further, that MPTP-treated monkeys treated with GDNF in these ways show a reduction in clinical scores and an improvement in motor behaviour (Sebastian et al. 2007).

Following on from these findings, the present study examined whether a neuroprotective agent, one that has been shown to enhance midbrain dopaminergic cell survival after parkinsonian insult, had any effect on the number of striatal TH$^+$ cells and GDNF expression. The neuroprotective agent we used was photobiomodulation (PBM) therapy (L = 670 nm). PBM has been shown to offer neuroprotection in cell culture (Liang et al. 2008; Ying et al. 2008; Trimmer et al. 2009), as well as in various insect (Vos et al. 2013; Powner et al. 2016), rodent (Whelan et al. 2008; Shaw et al. 2010, 2012; Peoples et al. 2012; Moro et al. 2013, 2014; Purushothuman et al. 2013; Johnstone et al. 2014; Reinhart et al. 2014, 2015; Oueslati et al. 2015; El Massri et al. 2016a) and monkey (Darlot et al. 2016; Moro et al. 2016; El Massri et al. 2016b) models of Parkinson's disease. In addition to neuroprotection, several studies have reported improved locomotor activity and a reduction in clinical signs after PBM (Whelan et al. 2008; Moro et al. 2013; Reinhart et al. 2014, 2015, 2016; Oueslati et al. 2015; Darlot et al. 2016). In the present study, we took the opportunity to examine our rodent (mouse: Moro et al. 2014; rat: Reinhart et al. 2015) and primate (monkey: Darlot et al. 2016) material further. These animals that had PBM via

an intracranial optical fibre device followed by either 6OHDA (rats) or MPTP (mice and monkeys) lesion.

Methods

Subjects

The striatum of Balb/c mice (*n* = 17; ~8 weeks old), Wistar rats (*n* = 15; ~8 weeks old) and macaque monkeys (Macaca fascicularis; *n* = 16; 4–5 years old) were analysed. Experiments were approved by the Animal Ethics Committee of the University of Sydney and COMETH (Grenoble), by the French Ministry for Research (protocol number 00562.02) and were performed in accordance with the European Communities Council Directive of 1986 (86/609/EEC) for care of laboratory animals.

Experimental procedure

We immunostained striatal and midbrain sections from animals used in previous studies (mouse: Moro et al. 2014; rat:; Reinhart et al. 2015; monkey:; Darlot et al. 2016). There was no overlap of results between the present study and those previous ones. Full details of the PBM optical fibre device and the entire experimental procedure were described in the previous studies, hence only the major points of protocol will be outlined here. Animals were implanted stereotactically with a PBM optical fibre (Fig. 1A′–C′). These fibres were attached proximally to a 670 nm laser diode, which was then connected to a battery. The lateral ventricle in mice (Fig. 1A″) and a midline region of the midbrain in rats (Fig. 1B″) and monkeys (Fig. 1C″) was targeted for implantation. Thereafter, the skull opening was covered with biological cement and the overlying tissues were sutured (Moro et al. 2014, 2016; Reinhart et al. 2015; Darlot et al. 2016). All implants were tested immediately before (arrow Fig. 1C′) and after implantation for efficacy.

MPTP and 6OHDA lesions

Mice had either two MPTP (ip, 25 mg/kg/injection; total of 50 mg/kg per mouse; Sigma) or saline injections over a 24 h period on 7 and 8 days post-surgery; this was followed by a 6 day survival period (Fig. 1a; Shaw et al. 2010, 2012; Moro et al. 2013, 2014; Johnstone et al. 2014; Reinhart et al. 2014, 2016; El Massri et al. 2016a). The monkeys received MPTP injections (im, 0.3 mg/kg/day) for 5 days (total of 1.5 mg/kg), from 14 to 18 days post surgery, followed by a 3 week survival period (Fig. 1c; Darlot et al. 2016). The control monkeys did not receive any injections (Control and PBM groups). For rats, 6OHDA (7.5 µg/µl)

or saline was injected stereotaxically into the caudate-putamen complex (CPu) of the right hand side (Heise and Mitrofanis 2005; Reinhart et al. 2015), immediately prior to optical fibre implantation (Reinhart et al. 2015).

Photobiomodulation (PBM)

For the mice and monkeys, the optical fibre device was turned-on during the period of MPTP (+saline in mice) injection. Soon after the last injection (6 h in mice and 24 h in monkeys), the device was turned-off (Fig. 1a, c). The output from the device was 0.16 mW power in mice (Moro et al. 2014) and 10 mW power in monkeys (Darlot et al. 2016). For the PBM-treated MPTP injected monkeys (MPTP-PBM group), these were from the group that showed few clinical signs and had evidence of neuroprotection (group 1; Darlot et al. 2016). We chose this group for inclusion because it would provide the clearest indication of whether PBM had an impact on striatal organisation after MPTP insult. In control monkeys, these had optical fibre implants and either the device never turned-on (Control group) or turned-on soon after surgery (PBM group). For the latter group, these animals had a slightly longer survival period (up to 12 weeks), hence providing a good indication of whether PBM alone had an impact on the internal striatal organisation. For rats, the optical fibre device was turned-on immediately after implantation (and soon after 6OHDA injection; see above), and remained on up until the end of the experimental period (Fig. 1b). The output from the device in rats was 0.16 mW power, the same as in mice (Reinhart et al. 2015). From previous measurements in body tissues, light signal has been detected up to 20–30 mm away from the source (Johnstone et al. 2016; Hamblin 2016). The striatum of mice and rats is certainly within the range of light signal from our midbrain (rats) or lateral ventricle (mice) implant sites (Paxinos and Franklin 2001; Paxinos and Watson 2005); in the larger brain of monkeys, the bulk of striatal tissue is still within range of our midbrain implant sites (Paxinos et al. 1998). Hence, we are confident that light signal reached most, if not all, the striatum in each species.

Immunohistochemistry and cell analysis

Animals had their brains aldehyde-fixed (4% buffered paraformaldehyde), cryoprotected and sectioned using a freezing microtome (mouse: Moro et al. 2014; rat: Reinhart et al. 2015; monkey: Darlot et al. 2016). Sections of striatum were incubated in either rabbit anti-TH (1:500; T8700 Sigma), anti-phosphorylated tyrosine hydroxylase S40 (THp40; 1:100; ab51206; Abcam), anti-phosphorylated tyrosine hydroxylase S31 (THp31; 1:100; ab51197; Abcam), anti-phosphorylated tyrosine hydroxylase

S19 (THp19; 1:100; ab51194; Abcam) or anti-GDNF (glial-derived neurotrophic factor; ab119473(1:500)/ab18956(1:50); Abcam and SCZSC-328(1:500); Santa Cruz). All sections were then incubated in biotinylated anti-rabbit IgG (ab64256, Abcam), followed by the streptavidin-peroxidase complex (ab64269, Abcam), reacted in a 3,3′-diaminobenzidine tetrahydrochloride solution (D3939 Sigma) and then finally coverslipped. Some midbrain sections were also processed using the THp antibodies, using the same protocol. For controls, sections were processed as described above except that no primary antibody was used. These control sections were immunonegative. As described by previous studies (Shaw et al. 2010, 2012; Peoples et al. 2012; Moro et al. 2013, 2014, 2016; Purushothuman et al. 2013; Johnstone et al. 2014; Reinhart et al. 2014, 2015, 2016; El Massri et al. 2016a, b; Darlot et al. 2016), the density of TH$^+$ terminals in the striatum was analysed using ImageJ software, while the number of TH$^+$ cells in the SNc and striatum, together with the number of THp40$^+$, THp31$^+$, THp19$^+$ cells in the striatum were estimated using the optical fractionator method (StereoInvestigator, MBF Science). For comparisons in the number of immunoreactive cells between groups, a one-way ANOVA test was performed, in-conjunction with multiple comparison tests (GraphPad Prism).

Western blots

We undertook western blots on the aldehyde-fixed striatal sections of monkeys. Ideally, we would have used fresh tissue, but this was not possible in our experimental paradigm. Nevertheless, with our use of controls and specific antibodies to GDNF and TH (Becker et al. 2007), we are confident that our western blots would detect any changes in the expression of these antigens induced by MPTP and/or PBM. The striatum was dissected away from sections in the PBM, MPTP and MPTP-PBM groups. Due to limited availability of primates for scientific use, we could only process sections from these groups, with the PBM group serving as our control. Protein was extracted using the Qproteome FFPE tissue kit (Qiagen) and total protein concentration of striatal tissue was calculated using a Bradford assay kit (Bio-Rad catalogue 500-0006). This was followed by running protein lysates on a 10%TGX Mini Protean Gel (Bio-Rad) then analysed using stain-free gel densitometry (Bio-Rad Image Lab software) to determine protein content. Western blots were run using the automated western blotting system Peggy Sue system (ProteinSimple). Samples with approximate equal amounts of protein were loaded onto a supplied well plate and incubated with either anti-TH (1:50; T8700 Sigma), anti-GAPDH (glyceraldehyde 3-phosphate dehydrogenase; loading control; 1:50;

ab9485; Abcam) or anti-GDNF (glial-derived neurotrophic factor; ab119473(1:50)/ab18956(1:50); Abcam and SCZSC-328(1:50); Santa Cruz), followed by biotinylated anti-rabbit IgG (ProteinSimple), followed by the streptavidin-peroxidase complex and ECL substrate for visualisation (ProteinSimple). Samples were run overnight. All analysis on samples (eg, area under curves and band intensity and size) were undertaken by the automated system within Peggy Sue. The experiment was run in triplicate and data for both TH and GDNF expression in each sample were normalised against GAPDH (loading control), and expressed as "relative expression" (Fig. 6d, e).

Results

In the section that follows, the results in mice, rats and monkeys will be considered separately.

Mice

We analysed striatal sections from four experimental groups of mice (Moro et al. 2014); Saline ($n = 5$), Saline-PBM ($n = 3$), MPTP ($n = 5$) and MPTP-PBM ($n = 4$). There were very few TH$^+$ cells in the striatum of mice; we estimated ~5000 cells across the entire striatum in controls (Fig. 2a), a value similar to that reported previously (Ünal et al. 2013). The majority of the striatal TH$^+$ cells had small somata (arrow Fig. 2c) that tended to be found in the dorsal regions of the nucleus. A minority of TH$^+$ cells had medium-sized somata (arrow Fig. 2d) and these were found mainly on the striatal border with the globus pallidus. When comparing between the different experimental groups, we found no major differences in the morphology nor number of striatal TH$^+$ cells (Fig. 2a; ANOVA: $F = 2.8$; $p > 0.05$). Further, no substantial differences were evident in the density of striatal TH$^+$ terminals between the groups (Fig. 2b; ANOVA: $F = 1.0$; $p > 0.05$).
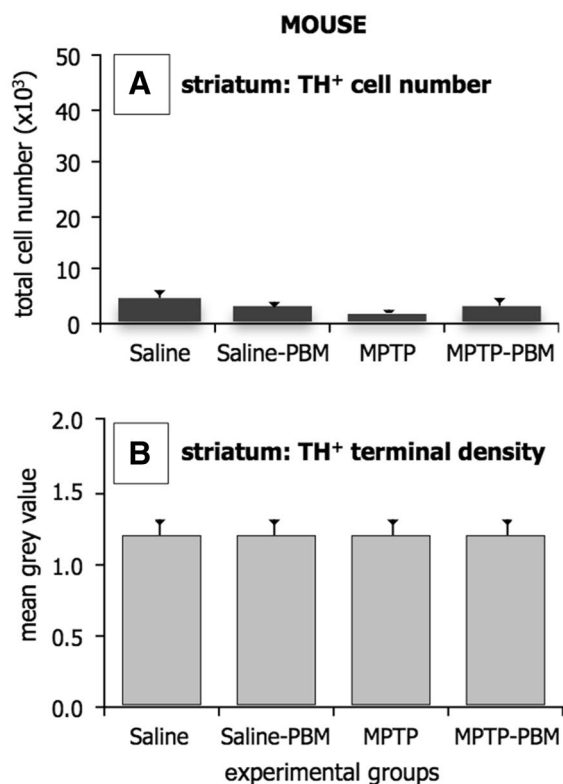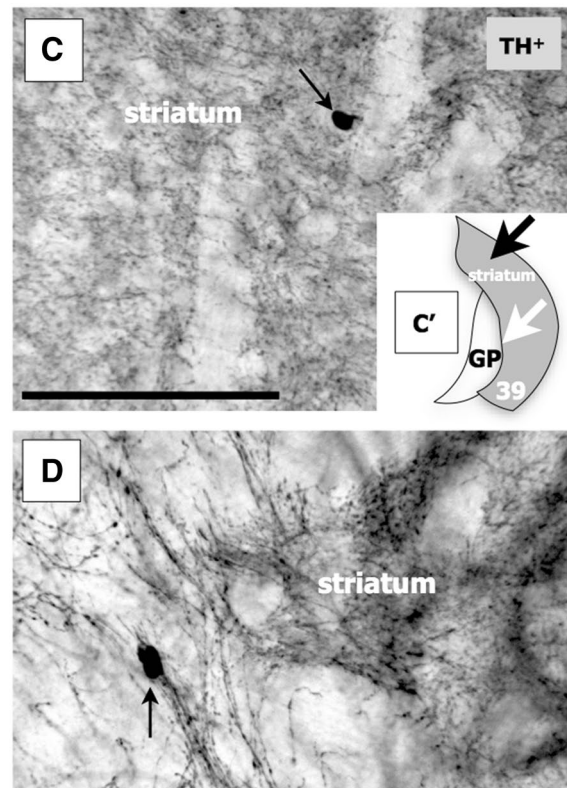

Fig. 2 Mice. Graphs showing **a** the estimated number of TH$^+$ cells in the striatum **b** the density of TH$^+$ terminals in the striatum of the different experimental groups. SEM are indicated for each column. **c** Photomicrograph of a small TH$^+$ cell (*arrow*) in the striatum. These cells were found mainly in the dorsal regions of the nucleus (*black arrow C'*). **d** Photomicrograph of a medium-sized TH$^+$ cell (*arrow*) in the striatum. These cells were found mainly on the striatal border with the globus pallidus (*white arrow C'*). Both examples are from the Saline group (other groups were similar; not shown). *Scale bar* 100 μm; both photomicrographs are of coronal sections, medial to *left* and dorsal to *top*

Rats

In rats, striatal sections from three experimental groups were analysed (Reinhart et al. 2015); Saline ($n = 5$), 6OHDA ($n = 5$) and 6OHDA-PBM ($n = 4$). As in mice, TH^{+} cells in the striatum of rats were not numerous; we estimated ~16,000 cells across the entire striatum of the Saline group (Fig. 3a). The majority of striatal TH^{+} cells had small somata (arrow Fig. 3c) and many were found in the dorsal regions of the nucleus. A minority of TH^{+} cells had medium-sized somata (arrow Fig. 3d) and these were found mainly on the striatal border with the globus pallidus. In some cases, the bulk of the dendritic tree of the medium-sized cells was evident, revealing their spiny profiles (arrowhead Fig. 3d). We found no major differences in the morphology of TH^{+} cells in the striatum of the different groups. In terms of number, although there were slightly more TH^{+} cells in both the 6OHDA and 6OHDA-PBM groups compared to the Saline group (Fig. 3a), these differences were found not significant (ANOVA: $F = 0.7$; $p > 0.05$). Further, we found no clear differences

in the overall density of striatal TH[+] terminals between the groups (Fig. 3b; ANOVA: $F = 0.2$; $p > 0.05$).

Monkey

We analysed striatal sections from four experimental groups of monkeys (Darlot et al. 2016); Control ($n = 3$), PBM ($n = 5$), MPTP ($n = 5$) and MPTP-PBM ($n = 3$). As in rodents, TH^{+} cells in the striatum of monkeys were not particularly numerous; in the control cases for example, we estimated ~500,000 cells across the entire striatum (Fig. 4a), a value similar to that reported previously (Palfi et al. 2002). The majority of striatal TH^{+} cells in monkeys had small somata (arrows Fig. 4d–f), while a minority had medium-sized somata (not shown; similar to that evident in rodents; Figs. 2d, 3d). We found no major differences in the morphology of TH^{+} cells in the striatum of the different groups (arrows Fig. 4d—f). In terms of number however, a clear pattern was evident. The number of striatal TH^{+} cells was similar in the Control and PBM groups and ~50% lower than in the MPTP group; in the MPTP-PBM
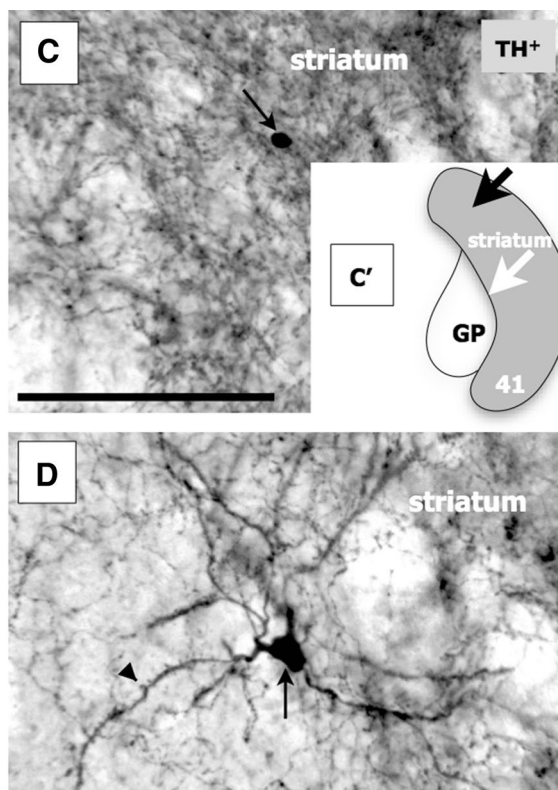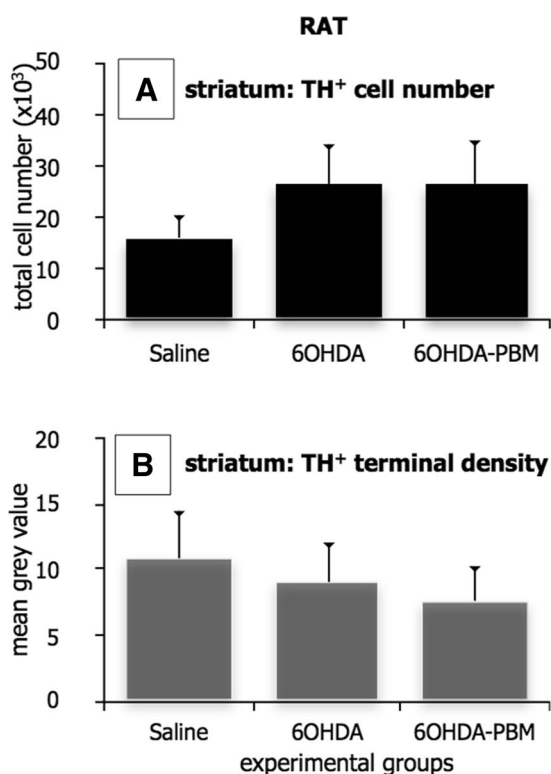

Fig. 3 Rats. Graphs showing **a** the estimated number of TH^{+} cells in the striatum **b** the density of TH[+] terminals in the striatum of the different experimental groups. SEM are indicated for each *column*. **c** Photomicrograph of a small TH[+] cell (*arrow*) in the striatum. These cells were found mainly in the dorsal regions of the nucleus (*black arrow C'*). **e** Photomicrograph of a medium-sized TH[+] cell (*arrow*)

in the striatum; the *arrowhead* indicates spines on dendrites. These cells were found mainly on the striatal border with the globus pallidus (*white arrow C'*). Both examples are from the Saline group (other groups were similar; not shown). *Scale bar* 100 μm; both photomicrographs are of coronal sections, medial to *left* and dorsal to *top*
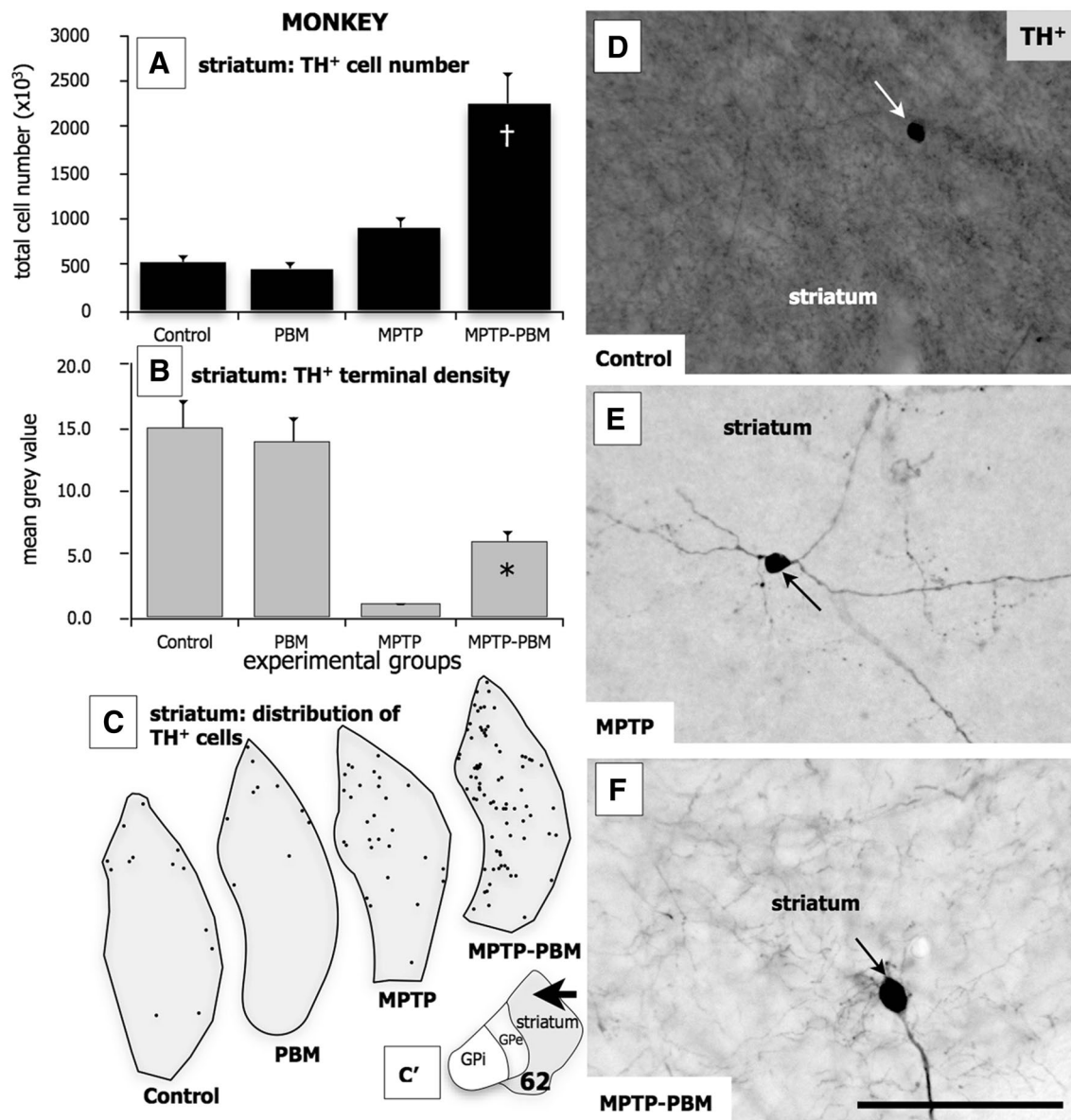
Fig. 4 Monkeys. Graphs showing **a** the estimated number of TH^{+} cells in the striatum **b** the density of TH[+] terminals in the striatum of the different experimental groups. SEM are indicated for each *column*. **c** Schematic diagrams of the distribution of TH^{+} cells in the striatum of the different experimental groups; sections were representative of pattern across entire striatum and correspond to plate 62 in monkey atlas (*C′*; Paxinos et al. 1998). Photomicrographs of small TH^{+} cells (*arrow*) in the striatum of the Control (**d**), MPTP (**e**) and MPTP-PBM (**f**) groups (such cells in PBM group were similar; not shown). *Arrow* in (*C′*) indicates approximate region were photomicrographs were taken from. *Scale bar* 100 μm; all photomicrographs are of coronal sections, medial to *left* and dorsal to *top*

group, quite strikingly, cell number was ~60% higher than in the MPTP group ($p > 0.001$) and ~80% higher than in the Control and PBM groups (Fig. 4a). These differences were significant (ANOVA: $F = 14$; $p < 0.0001$). Figure 4c shows the distribution of TH^{+} cells from representative sections in the Control, PBM, MPTP and MPTP-PBM groups. In each group, TH^{+} cells were found across all regions of the striatum, with a tendency for more cells to be located dorsally than ventrally (Palfi et al. 2002). Other than the differences in number, there was no clear evidence for a difference in the distribution of TH^{+} cells between the different groups (Fig. 4c). In terms of TH[+] terminals in the striatum, there was a reduction in density in both the MPTP and MPTP-PBM groups compared to the Control and PBM groups (Fig. 4b; ANOVA: $F = 32$; $p < 0.0001$). Although the reduction from controls was massive in both groups, it was clearly less in the MPTP-PBM compared to the MPTP group ($p < 0.05$).

We next examined the patterns of THp40, THp31 and THp19 immunoreactivity in this species. All these antibodies labelled cells similar in morphology to the small TH$^+$ cells described above, except that THp40, THp31 and THp19 immunoreactivity tended to be localised within the soma and not, or rarely, within the dendrites (arrows Fig. 5a, c, d). THp40 immunoreactivity was seen also in many axonal profiles within the striatum (arrowhead Fig. 5b), while THp31 and THp19 immunoreactivity was not evident in these profiles (Fig. 5c, d). Figure 5e shows that there were few THp40$^+$, THp31$^+$ and THp19$^+$ cells seen in the striatum of the different groups. The differences

in the estimated total number of THp40$^+$, THp31$^+$ and THp19$^+$ between the groups were not significant (ANOVA: $F = 3.3$; $p > 0.05$). Unlike in the striatum, there was rich THp40 (arrow Fig. 5f), THp31 (arrow Fig. 5g) and THp19 (arrow Fig. 5h) immunoreactivity in the SNc, particularly its dorsal sector, in monkeys of all the groups.

We then examined the patterns of GDNF expression in this species. We found very few GDNF$^+$ cells in the striatum of each group from immunohistochemical sections (Palfi et al. 2002; Sebastian et al. 2007). This was the case with the three commercially available antibodies to GDNF that we used (see "Methods"). On the rare occasion when
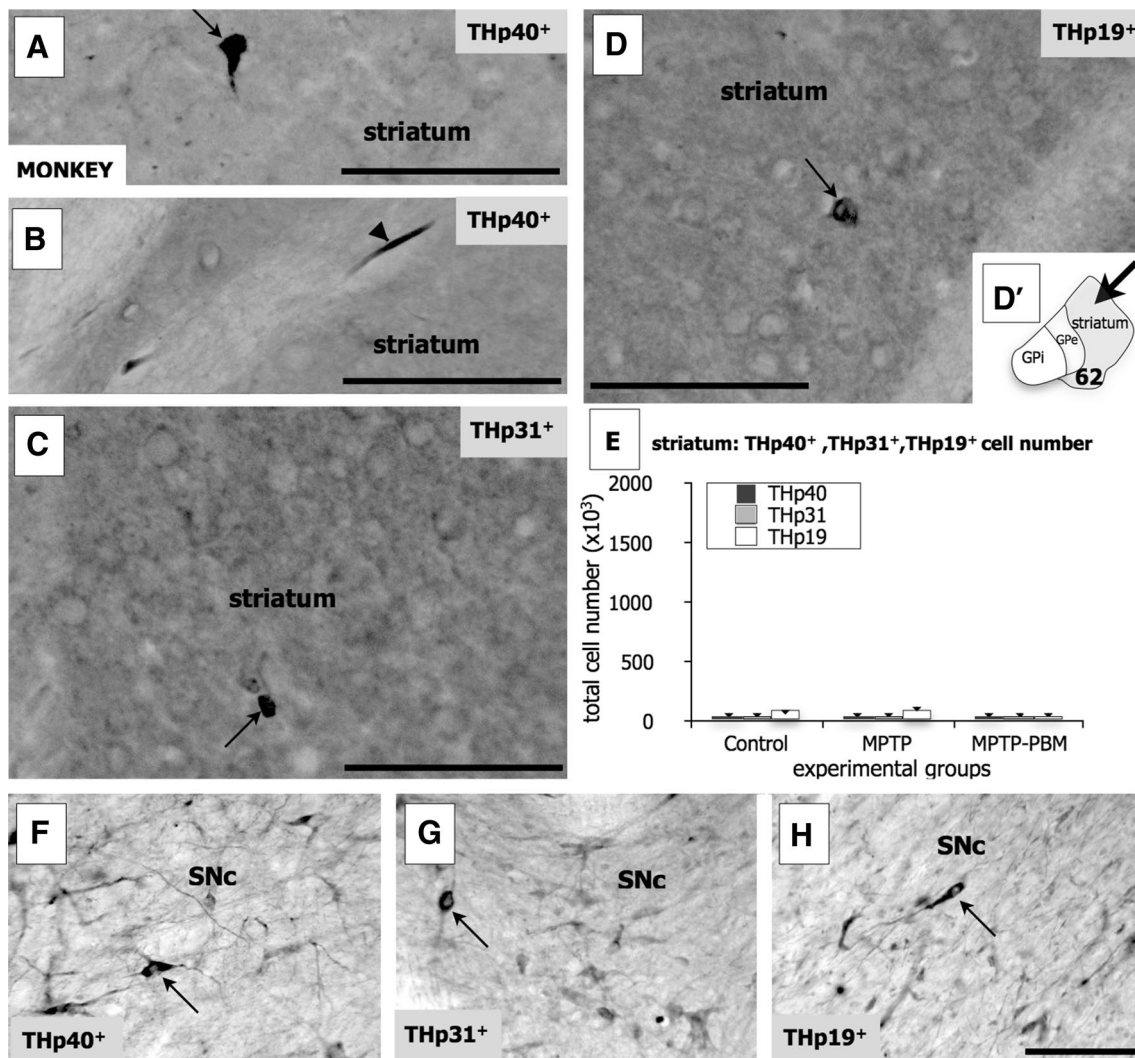

Fig. 5 Monkeys. Photomicrographs of **a, b** THp40 **c** THp31 and **d** THp19 immunoreactivity in the striatum. These examples are from the MPTP group (other groups were similar; not shown). The bulk of THp40$^+$ (**a**) THp31$^+$ (**b**) THp19$^+$ (**c**) cells had small somata and immunoreactivity was largely limited to the somata (*arrows*). *Arrow* in (*D'*) indicates approximate region were photomicrographs were taken from (corresponding to plate 62 in monkey atlas; Paxinos et al. 1998). **e** *Graph* showing the estimated number of THp40$^+$, THp31$^+$,

THp19$^+$ cells in the striatum of the different experimental groups. SEM are indicated for each column. Photomicrographs of THp40 (*arrow* **f**), THp31 (*arrow* **g**) and THp19 (*arrow* **h**) immunoreactivity in the SNc. These cells were in the dorsal sector of the nucleus. These examples are from the MPTP group (other groups were similar; not shown). *Scale bar* 100 μm; all photomicrographs are of coronal sections, medial to *left* and dorsal to *top*

we did find immunoreactive cells in the striatum, they were small and immunoreactivity was limited to the somata (arrows Fig. 6a, b). We hence moved to western blots to explore GDNF expression further. Using this method, we found clear GDNF[+] bands in each of the three groups analysed (Fig. 6c; ANOVA: $F = 7.7$; $p < 0.05$). There was an
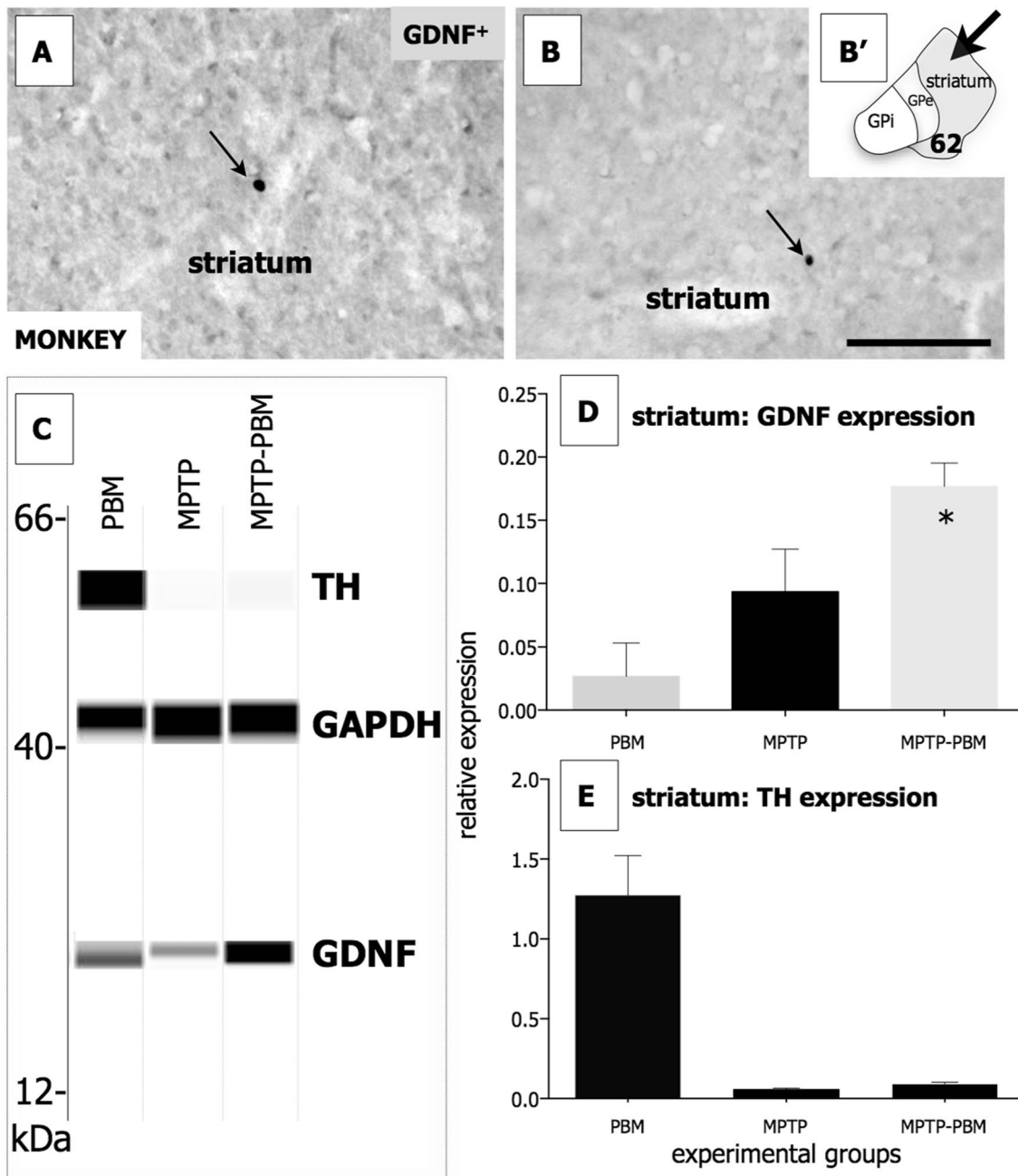

Fig. 6 Monkeys. Photomicrographs of (**a, b** *arrows*) GDNF^{+} cells in the striatum. These examples are from the MPTP group (other groups were similar; not shown). Very few labelled cells were seen in any given section; in fact, many of the sections of each animal were barren of labelled cells. When they were found, they had small somata and immunoreactivity was largely limited to the somata (*arrows*). *Scale bar* 100 μm; all photomicrographs are of coronal sections, medial to *left* and dorsal to *top*. Arrow in *B'* indicates approximate region were photomicrographs were taken from (corresponding to plate 62 in monkey atlas; Paxinos et al. 1998). **c** Examples of western blots for TH, GDNF (similar band patterns were seen from the three antibodies used) and GAPDH (loading control) from samples of the three groups analysed. **d** Graph showing GDNF expression normalised against the loading control GAPDH (relative expression) in the three groups analysed; *in MPTP-PBM group column represents significant difference ($p < 0.05$) to MPTP group. **e** Graph showing TH expression normalised against the loading control GAPDH (relative expression) in the three groups analysed. SEM are indicated for each column

~35% increase in expression (when normalised against the loading control, GAPDH) in the MPTP compared to the control PBM group (Fig. 6d); in the MPTP-PBM group, there was a further ~50% increase in expression from the MPTP group ($p < 0.05$), and an ~85% increase from the control PBM group ($p < 0.001$). We also explored the patterns of TH expression in the different groups using western blots. As seen from the immunohistochemical sections (Fig. 4b), the western blots indicated a massive reduction in TH expression in the striatum of both the MPTP and MPTP-PBM groups, compared to the control PBM groups (Fig. 6e). From the western blots, there was a slightly higher expression of TH in the MPTP-PBM compared to the MPTP group (Fig. 6e), but unlike the immunohistochemistry (Fig. 4b), this increase did not reach statistical significance ($p > 0.05$).

Discussion

We found that PBM therapy had a major impact on the number of TH^{+} cells and patterns of GDNF expression in the deafferentated striatum of MPTP-treated monkeys. Our results indicate the striatum as a potential therapeutic target for PBM therapy in Parkinson's disease.

Changes in striatal TH[+] cell number is dependent on a loss of dopaminergic terminations?

Previous studies have reported that the number of striatal TH^{+} cells is related closely to the density of TH[+] terminals and dopaminergic transmission (Betarbet et al. 1997; Porritt et al. 2000; Palfi et al. 2002; Cossette et al. 2005; Huot et al. 2007). For example, in MPTP-treated monkeys (Huot et al. 2008), 6OHDA-lesioned mice (Darmopil et al. 2008) and Parkinson's disease patients (Huot et al. 2007), L-dopa administration results in little or no increase in the number of striatal TH^{+} cells. The results of the present study are consistent with these previous findings. In our monkey model, where there was a marked loss of striatal TH[+] terminations in animals, there was a clear increase in the number of striatal TH^{+} cells. By contrast, in our mouse and rat models, where the overall loss of striatal TH[+] terminations was minimal, there was no clear increase in striatal TH[+] cell number. In other rodent models that result in larger MPTP and 6OHDA lesions, both of which would reduce the overall density of striatal TH[+] terminations, an increase in striatal TH[+] cell number has been reported (Meredith et al. 1999; Darmopil et al. 2008; Ünal et al. 2013; Depboylu 2014; Xenias et al. 2015). For our purposes here, the patterns evident in the striatum of our mouse and rat model provide for an excellent contrast to the patterns evident in the striatum of our monkey model. In particular, that an increase in striatal TH[+] cell number results after a large decrease in striatal TH[+] terminations.

The increase in striatal TH[+] cell number after striatal deafferentation is thought to be an intrinsic compensatory mechanism, in an effort to restore dopamine neurotransmission (Betarbet et al. 1997; Porritt et al. 2000; Palfi et al. 2002; Cossette et al. 2005; Huot et al. 2007). It is not entirely clear however, if these cells are capable of making dopamine, at least in sufficient quantities to make up for that loss after deafferentation of the striatum. Many cells, for example, appear to lack all of the enzymes required to make dopamine in mice, and perhaps also in monkeys (see "Introduction"). Our findings in monkeys, as with those in mice (Depboylu 2014), indicated that many of the striatal TH^{+} cells did not express phosphorylated TH (S40, S31 and S19), suggesting that they are likely to have a low activity of TH. It is not clear whether this seemingly low TH activity is sufficient to increase dopaminergic transmission in the deafferented striatum, and indeed make for a clinical and functional difference.

Photobiomodulation stimulates TH and GDNF expression in the monkey striatum

We found that, while the monkeys in the MPTP group had more TH^{+} cells (Betarbet et al. 1997; Porritt et al. 2000; Palfi et al. 2002; Cossette et al. 2005; Huot et al. 2007) and GDNF expression than the controls, the MPTP-PBM group had even more striatal TH^{+} cells (~60%) and GDNF expression (~50%) than the MPTP group. PBM of the deafferentated monkey striatum appeared to stimulate the intrinsic compensatory mechanisms even more (see above). Such increases were not evident in the control PBM group (and in our mouse and rat models; see above), indicating that a striatal lesion was required before PBM triggered the intrinsic compensatory mechanisms. It should be noted that, although the MPTP-PBM group had more striatal TH[+] terminations than the MPTP group, it still had many fewer terminations than the PBM (+control) group (Fig. 4b); the MPTP-PBM group still, in effect, had a striatal lesion, seemingly sufficient for PBM to induce both TH and GDNF expression.

The PBM-induced increase in GDNF expression is of particular interest. Previous studies have shown that GDNF (Gash et al. 2005; Orme et al. 2013), together with others such as acidic fibroblast growth factor (aFGF; Du and Iacovitti 1997; Du et al. 1995) and brain-derived neurotrophic factor (BDNF; Du et al. 1995), increase the number of TH^{+} cells in cell culture and in the SNc. Further, in vivo application of GDNF (Palfi et al. 2002; Sebastian et al. 2007) or FGF (Jollivet et al. 2004), results in a large increase in striatal TH[+] cell number after parkinsonian insult, in patterns similar to that observed after our PBM treatment
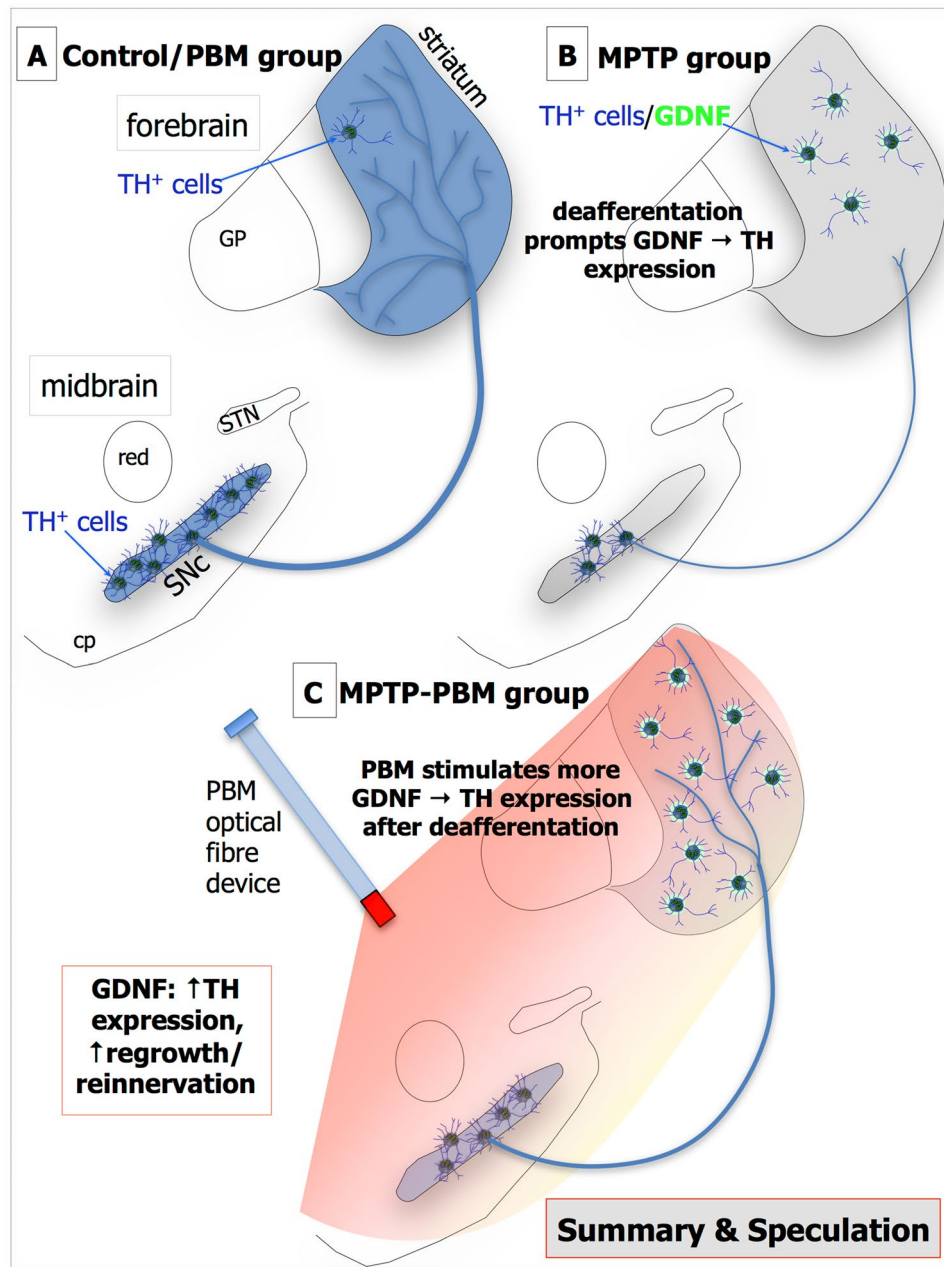
Fig. 7 Summary and speculation of the patterns of TH and GDNF expression in the striatum in **a** controls (control and PBM group). **b** MPTP-treated (MPTP group) and **c** MPTP-treated exposed to PBM (MPTP-PBM group). In the controls (**a**), there are many TH+ cells in the SNc and they have rich terminations in the striatum; there are very few striatal TH+ cells in these cases. After MPTP treatment (**b**), there are fewer TH+ cells in the SNc and the striatum is largely deafferentated, almost barren of TH+ terminations. Contrary to these losses, there is a clear increase in striatal TH+ cell number after MPTP lesion. There is also an increase in GDNF expression in the striatum, presumably within the cells themselves, and this expression is thought to trigger the TH expression (see text for details). Hence, the MPTP lesion or deafferentation appears to prompt intrinsic compensatory mechanisms within the striatum. In the MPTP-treated cases that were exposed to PBM also (**c**), there is an increase in TH+ cell number in the SNc, to near control levels; within the striatum, there is an increase in TH+ terminations in these cases, although nowhere near to control-like levels. PBM appears to stimulate a further increase in GDNF expression in the MPTP-lesioned striatum, triggering the expression of TH in more striatal cells. We suggest that PBM, after MPTP lesion or deafferentation, prompts the striatal intrinsic compensatory mechanisms even further

(see above). We suggest that PBM stimulated the expression of GDNF which, in turn, switched-on TH expression in striatal cells; that the PBM-induced increase in striatal TH+ cell number was mediated by GDNF. It remains to be determined whether the PBM-induced GDNF expression in the striatum derives from the neurones and/or the

surrounding glia, in particular astrocytes (Sandhu et al. 2009; d'Angelmont et al. 2015).

Recent studies have reported that PBM is associated with the up-regulation of another trophic factor, namely BDNF. PBM stimulates an increase in BDNF expression after traumatic brain injury (Xuan et al. 2013), together with increasing dendritic morphogenesis and neural connectivity in embryonic rats (Meng et al. 2013). In fact, BDNF, together with GDNF, have been shown to be expressed in the striatum of 6OHDA-lesioned rats after of injection viral vectors (Sun et al. 2005). Both trophic factors were shown effective in improving behaviour and offering neuroprotection. In relation to our study here, PBM may not only induce GDNF expression in the parkinsonian striatum, but other factors, such as BDNF, as well (Hamblin 2016).

It should be noted that transcranial application of PBM in both rodents and monkeys is likely to have an effect on TH and GDNF expression in the striatum as well, similar to that described here for intracranial midbrain application. The striatum in both rodents (mouse 2–3 mm; rat 4–5 mm) and monkeys (15–20 mm) is near enough to the cranial surface for the externally applied light to reach it. In humans, the striatum is much further away from the cranial surface (50–60 mm), beyond the reach of light applied externally (see Johnstone et al. 2016). For these reasons, with the human application in mind, we have developed the intracranial approach, not only for PBM to reach the midbrain, but the striatum as well.

Significance of PBM-induced TH and GDNF expression after MPTP treatment

Taken all the results together, we would like to speculate on the following scenario. In the MPTP-deafferentated striatum, interneurones—as an intrinsic compensatory mechanism—produce GDNF that triggers TH expression (Fig. 7). PBM appears to stimulate these mechanisms further, prompting more GDNF expression (and perhaps other trophic factors as well), leading to increased TH expression in cells (Fig. 7c). In addition, we suggest that GDNF has a more global role in the deafferentated striatum, serving as a trophic sign post and actively promoting the regrowth and reinnervation of dopaminergic axons within the striatum. All in all, the beneficial intrinsic compensatory mechanisms of the striatum - triggered in response to deafferentation - may be enhanced further by PBM.

Conclusions

Our results showed that, after deafferentation of the monkey striatum, PBM-induced an increase in the number of striatal TH^{+} cells, together with the well-known trophic factor, GDNF. We suggest that the PBM-induced GDNF expression stimulated the expression of TH in new cells and has a trophic function, encouraging the regrowth of axons and reinnervation of cellular targets in the striatum. More broadly, the induction of GDNF expression and perhaps other trophic factors also, may in fact be a means by which PBM elicits its beneficial effects across neural tissues. Overall, our results raise the idea of a new therapeutic direction, one linking PBM with GDNF expression and its trophic effects. It also highlights the striatum as a potential therapeutic target for PBM therapy.

References

Becker K-F, Schott C, Hipp S et al (2007) Quantitative protein analysis from formalin-fixed tissues: implications for translational clinical research and nanoscale molecular diagnosis. J Pathol 211:370–378. doi:10.1002/path.2107

Betarbet R, Turner R, Chockkan V et al (1997) Dopaminergic neurons intrinsic to the primate striatum. J Neurosci 17:6761–6768

Blandini F, Nappi G, Tassorelli C, Martignoni E (2000) Functional changes of the basal ganglia circuitry in Parkinson's disease. Prog Neurobiol 62:63–88

Cossette M, Lecomte F, Parent A (2005) Morphology and distribution of dopaminergic neurons intrinsic to the human striatum. J Chem Neuroanat 29:1–11. doi:10.1016/j.jchemneu.2004.08.007

d'Anglemont de Tassigny X, Pascual A, López-Barneo J (2015) GDNF-based therapies, GDNF-producing interneurons, and trophic support of the dopaminergic nigrostriatal pathway. Implications for Parkinson's disease. Front Neuroanat 9:10. doi:10.3389/fnana.2015.00010

Darlot F, Moro C, El Massri N et al (2016) Near-infrared light is neuroprotective in a monkey model of Parkinson disease. Ann Neurol 79:59–75. doi:10.1002/ana.24542

Darmopil S, Muñetón-Gómez VC, de Ceballos ML et al (2008) Tyrosine hydroxylase cells appearing in the mouse striatum after dopamine denervation are likely to be projection neurones regulated by L-DOPA. Eur J Neurosci 27:580–592. doi:10.1111/j.1460-9568.2008.06040.x

Depboylu C (2014) Non-serine-phosphorylated tyrosine hydroxylase expressing neurons are present in mouse striatum, accumbens and cortex that increase in number following dopaminergic denervation. J Chem Neuroanat 56:35–44. doi:10.1016/j.jchemneu.2014.02.001

Du X, Iacovitti L (1997) Multiple signaling pathways direct the initiation of tyrosine hydroxylase gene expression in cultured brain neurons. Brain Res Mol Brain Res 50:1–8

Du X, Stull ND, Iacovitti L (1995) Brain-derived neurotrophic factor works coordinately with partner molecules to initiate tyrosine hydroxylase expression in striatal neurons. Brain Res 680:229–233

Dubach M, Schmidt R, Kunkel D et al (1987) Primate neostriatal neurons containing tyrosine hydroxylase: Immunohistochemical evidence. Neurosci Lett 75:205–210. doi:10.1016/0304-3940(87)90298-9

El Massri N, Johnstone DM, Peoples CL et al (2016a) The effect of different doses of near infrared light on dopaminergic cell survival and gliosis in MPTP-treated mice. Int J Neurosci 126:76–87. doi:10.3109/00207454.2014.994063

El Massri N, Moro C, Torres N et al (2016b) Near-infrared light treatment reduces astrogliosis in MPTP-treated monkeys. Exp Brain Res 1–8. doi:10.1007/s00221-016-4720-7

Gash DM, Zhang Z, Ai Y et al (2005) Trophic factor distribution predicts functional recovery in parkinsonian monkeys. Ann Neurol 58:224–233. doi:10.1002/ana.20549

Hamblin MR (2016) Shining light on the head: Photobiomodulation for brain disorders. BBA Clin 6:113–124. doi:10.1016/j.bbacli.2016.09.002

Heise CE, Mitrofanis J (2005) Reduction in parvalbumin expression in the zona incerta after 6OHDA lesion in rats. J Neurocytol 34:421–434. doi:10.1007/s11068-006-8728-y

Huot P, Lévesque M, Parent A (2007) The fate of striatal dopaminergic neurons in Parkinson's disease and Huntington's chorea. Brain 130:222–232. doi:10.1093/brain/awl332

Huot P, Lévesque M, Morissette M et al (2008) L-Dopa treatment abolishes the numerical increase in striatal dopaminergic neurons in parkinsonian monkeys. J Chem Neuroanat 35:77–84. doi:10.1016/j.jchemneu.2007.06.004

Johnstone DM, El Massri N, Moro C et al (2014) Indirect application of near infrared light induces neuroprotection in a mouse model of parkinsonism—an abscopal neuroprotective effect. Neuroscience 274:93–101. doi:10.1016/j.neuroscience.2014.05.023

Johnstone DM, Moro C, Stone J et al (2016) Turning on lights to stop neurodegeneration: the potential of near infrared light therapy in Alzheimer's and Parkinson's disease. Front Neurosci 9:500. doi:10.3389/fnins.2015.00500

Jollivet C, Montero-Menei CN, Venier-Julienne M-C et al (2004) Striatal tyrosine hydroxylase immunoreactive neurons are induced by L-dihydroxyphenylalanine and nerve growth factor treatment in 6-hydroxydopamine lesioned rats. Neurosci Lett 362:79–82. doi:10.1016/j.neulet.2004.02.068

Liang HL, Whelan HT, Eells JT, Wong-Riley MTT (2008) Near-infrared light via light-emitting diode treatment is therapeutic against rotenone- and 1-methyl-4-phenylpyridinium ion-induced neurotoxicity. Neuroscience 153:963–974. doi:10.1016/j.neuroscience.2008.03.042

Mazloom M, Smith Y (2006) Synaptic microcircuitry of tyrosine hydroxylase-containing neurons and terminals in the striatum of 1-methyl-4-phenyl-1,2,3,6-tetrahydropyridine-treated monkeys. J Comp Neurol 495:453–469. doi:10.1002/cne.20894

Meng C, He Z, Xing D (2013) Low-level laser therapy rescues dendrite atrophy via upregulating BDNF expression: implications for Alzheimer's Disease. J Neurosci 33:13505–13517. doi:10.1523/JNEUROSCI.0918-13.2013

Meredith GE, Farrell T, Kellaghan P et al (1999) Immunocytochemical characterization of catecholaminergic neurons in the rat striatum following dopamine-depleting lesions. Eur J Neurosci 11:3585–3596. doi:10.1046/j.1460-9568.1999.00774

Moro C, Torres N, El Massri N et al (2013) Photobiomodulation preserves behaviour and midbrain dopaminergic cells from MPTP toxicity: evidence from two mouse strains. BMC Neurosci 14:40. doi:10.1186/1471-2202-14-40

Moro C, El Massri N, Torres N et al (2014) Photobiomodulation inside the brain: a novel method of applying near-infrared light intracranially and its impact on dopaminergic cell survival in MPTP-treated mice. J Neurosurg 120:670–683. doi:10.3171/2013.9.JNS13423

Moro C, El Massri N, Darlot F, et al (2016) Effects of a higher dose of near-infrared light on clinical signs and neuroprotection in a monkey model of Parkinson's disease. Brain Res 1648 Part A 19–26. doi:10.1016/j.brainres.2016.07.005

Orme RP, Bhangal MS, Fricker RA (2013) Calcitriol imparts neuroprotection in vitro to midbrain dopaminergic neurons by upregulating GDNF expression. PLoS One. doi:10.1371/journal.pone.0062040

Oueslati A, Lovisa B, Perrin J et al (2015) Photobiomodulation suppresses alpha-synuclein-induced toxicity in an AAV-based rat genetic model of Parkinson's disease. PLoS One 10:e0140880. doi:10.1371/journal.pone.0140880

Palfi S, Leventhal L, Chu Y et al (2002) Lentivirally delivered glial cell line-derived neurotrophic factor increases the number of striatal dopaminergic neurons in primate models of nigrostriatal degeneration. J Neurosci 22:4942–4954

Parent A, Hazrati L-N (1995) Functional anatomy of the basal ganglia. I. The cortico-basal ganglia-thalamo-cortical loop. Brain Res Rev 20:91–127. doi:10.1016/0165-0173(94)00007-C

Paxinos G, Franklin K (2001) The mouse brain in stereotaxic coordinates, 2nd edn. Academic press, California, USA

Paxinos G, Watson CR (2005) The rat brain in stereotaxic coordinates, 5th edn. Elsevier Academic Press, Amsterdam, Boston

Paxinos G, Huang X, Toga A (1998) The Rhesus monkey brain in stereotaxic coordinates. Academic Press, USA

Peoples C, Spana S, Ashkan K et al (2012) Photobiomodulation enhances nigral dopaminergic cell survival in a chronic MPTP mouse model of Parkinson's disease. Parkinsonism Relat Disord 18:469–476. doi:10.1016/j.parkreldis.2012.01.005

Porritt MJ, Batchelor PE, Hughes AJ et al (2000) New dopaminergic neurons in Parkinson's disease striatum. The Lancet 356:44–45. doi:10.1016/S0140-6736(00)02437-5

Powner MB, Salt TE, Hogg C, Jeffery G (2016) Improving mitochondrial function protects bumblebees from neonicotinoid pesticides. PLOS One 11:e0166531. doi:10.1371/journal.pone.0166531

Purushothuman S, Nandasena C, Johnstone DM et al (2013) The impact of near-infrared light on dopaminergic cell survival in a transgenic mouse model of parkinsonism. Brain Res 1535:61–70. doi:10.1016/j.brainres.2013.08.047

Reinhart F, Massri NE, Darlot F et al (2014) 810 nm near-infrared light offers neuroprotection and improves locomotor activity in MPTP-treated mice. Neurosci Res. doi:10.1016/j.neures.2014.11.005

Reinhart F, El Massri N, Darlot F et al (2015) Evidence for improved behaviour and neuroprotection after intracranial application of near infrared light in a hemi-parkinsonian rat model. J Neurosurg 27:1–13

Reinhart F, El Massri N, Johnstone DM et al (2016) Near-infrared light (670 nm) reduces MPTP-induced parkinsonism within a broad therapeutic time window. Exp Brain Res. doi:10.1007/s00221-016-4578-8

Sandhu JK, Gardaneh M, Iwasiow R et al (2009) Astrocyte-secreted GDNF and glutathione antioxidant system protect neurons against 6OHDA cytotoxicity. Neurobiol Dis 33:405–414. doi:10.1016/j.nbd.2008.11.016

Sebastián WS, Guillén J, Manrique M et al (2007) Modification of the number and phenotype of striatal dopaminergic cells by carotid body graft. Brain 130:1306–1316. doi:10.1093/brain/awm061

Shaw VE, Spana S, Ashkan K et al (2010) Neuroprotection of midbrain dopaminergic cells in MPTP-treated mice after

near-infrared light treatment. J Comp Neurol 518:25–40. doi:10.1002/cne.22207

Shaw VE, Peoples C, Spana S et al (2012) Patterns of cell activity in the subthalamic region associated with the neuroprotective action of near-infrared light treatment in MPTP-Treated mice. Parkinsons Dis 296875. doi:10.1155/2012/296875

Sun M, Kong L, Wang X et al (2005) Comparison of the capability of GDNF, BDNF, or both, to protect nigrostriatal neurons in a rat model of Parkinson's disease. Brain Res 1052:119–129. doi:10.1016/j.brainres.2005.05.072

Tandé D, Höglinger G, Debeir T et al (2006) New striatal dopamine neurons in MPTP-treated macaques result from a phenotypic shift and not neurogenesis. Brain 129:1194–1200. doi:10.1093/brain/awl041

Tashiro Y, Sugimoto T, Hattori T et al (1989) Tyrosine hydroxylase-like immunoreactive neurons in the striatum of the rat. Neurosci Lett 97:6–10. doi:10.1016/0304-3940(89)90130-4

Trimmer PA, Schwartz KM, Borland MK et al (2009) Reduced axonal transport in Parkinson's disease cybrid neurites is restored by light therapy. Mol Neurodegener 4:26. doi:10.1186/1750-1326-4-26

Ünal B, Shah F, Kothari J, Tepper JM (2013) Anatomical and electrophysiological changes in striatal TH interneurons after loss of the nigrostriatal dopaminergic pathway. Brain Struct Funct 220:331–349. doi:10.1007/s00429-013-0658-8

Vos M, Lovisa B, Geens A et al (2013) Near-Infrared 808 nm light boosts complex IV-dependent respiration and rescues a Parkinson-related pink1 model. PLoS One 8:e78562. doi:10.1371/journal.pone.0078562

Weihe E, Depboylu C, Schütz B et al (2006) Three types of tyrosine hydroxylase-positive CNS neurons distinguished by dopa decarboxylase and VMAT2 co-expression. Cell Mol Neurobiol 26:659–678. doi:10.1007/s10571-006-9053-9

Whelan HT, DeSmet KD, Buchmann EV et al (2008) Harnessing the cell's own ability to repair and prevent neurodegenerative disease. SPIE Newsroom 24:1–3

Xenias HS, Ibáñez-Sandoval O, Koós T, Tepper JM (2015) Are striatal tyrosine hydroxylase interneurons dopaminergic? J Neurosci 35:6584–6599. doi:10.1523/JNEUROSCI.0195-15.2015

Xuan W, Vatansever F, Huang L et al (2013) Transcranial low-level laser therapy improves neurological performance in traumatic brain injury in mice: effect of treatment repetition regimen. PLoS One 8:e53454. doi:10.1371/journal.pone.0053454

Ying R, Liang HL, Whelan HT et al (2008) Pretreatment with near-infrared light via light-emitting diode provides added benefit against rotenone- and MPP+-induced neurotoxicity. Brain Res 1243:167–173. doi:10.1016/j.brainres.2008.09.057